IOP Publishing Smart Materials and Structures
Smart Mater. Struct. 25 (2016) 105005 (15pp) doi:10.1088/0964-1726/25/10/105005

Electrical percolation threshold of cementitious composites possessing self-sensing functionality incorporating different carbon-based materials

Ali Al-Dahawi[1,2], Mohammad Haroon Sarwary[3], Oğuzhan Öztürk[4], Gürkan Yıldırım[5], Arife Akın[4], Mustafa Şahmaran[3] and Mohamed Lachemi[6]

[1] Department of Civil Engineering, Gaziantep University, Gaziantep, Turkey
[2] Department of Building and Construction Engineering, University of Technology, Baghdad, Iraq
[3] Department of Civil Engineering, Gazi University, Ankara, Turkey
[4] Department of Civil Engineering, Selçuk University, Konya, Turkey
[5] Department of Civil Engineering, Adana Science and Technology University, Adana, Turkey
[6] Department of Civil Engineering, Ryerson University, Toronto, Canada

E-mail: gyildirim@adanabtu.edu.tr and gurkanyildirimgy@gmail.com

Received 26 March 2016, revised 26 July 2016
Accepted for publication 25 August 2016
Published 16 September 2016

Abstract

An experimental study was carried out to understand the electrical percolation thresholds of different carbon-based nano- and micro-scale materials in cementitious composites. Multi-walled carbon nanotubes (CNTs), graphene nanoplatelets (GNPs) and carbon black (CB) were selected as the nano-scale materials, while 6 and 12 mm long carbon fibers (CF6 and CF12) were used as the micro-scale carbon-based materials. After determining the percolation thresholds of different electrical conductive materials, mechanical properties and piezoresistive properties of specimens produced with the abovementioned conductive materials at percolation threshold were investigated under uniaxial compressive loading. Results demonstrate that regardless of initial curing age, the percolation thresholds of CNT, GNP, CB and CFs in ECC mortar specimens were around 0.55%, 2.00%, 2.00% and 1.00%, respectively. Including different carbon-based conductive materials did not harm compressive strength results; on the contrary, it improved overall values. All cementitious composites produced with carbon-based materials, with the exception of the control mixtures, exhibited piezoresistive behavior under compression, which is crucial for sensing capability. It is believed that incorporating the sensing attribute into cementitious composites will enhance benefits for sustainable civil infrastructures.

Keywords: engineered cementitious composites (ECC), self-sensing, piezoresistivity, percolation threshold, carbon-based materials

(Some figures may appear in colour only in the online journal)

1. Introduction

Concrete-like cementitious materials are regarded as 'multi-functional' when they exhibit functional characteristics in addition to basic structural properties. Generally speaking, structural materials that do not contain sensory material but are used for sensing are called 'self-sensing' materials. Thanks to the ease of modifying concrete-like cementitious materials with self-sensing ability, structural/materials health monitoring can easily be implemented without requiring complex integrated systems. The complexity of integrated systems arises from the difficulty of combining disparate high-performance material/structural systems, structural health monitoring systems and functionality monitoring

systems. However, it is possible to develop smart, multi-functional materials that combine three different systems into one body and address all the desired tasks.

Over the last few decades, multifunctional smart structural materials—which are sensitive and responsive to certain stimuli—have been investigated. They are regarded as next-generation construction materials that combine mechanical and functional properties simultaneously (Chung 2002, 2003, Wen and Chung 2005, 2006, 2008, Perez *et al* 2010, Zornoza *et al* 2010, Baeza *et al* 2013). One potentially promising material that can interconnect self-sensing ability and superior mechanical properties is engineered cementitious composites (ECCs) (Li 2002). Although the composition of ECC is similar to both conventional concrete and fiber reinforced concrete, the material distinguishes itself with superior tensile properties with tensile strain capacity of more than 3% under uniaxial tensile loading (about more than 300 times that of normal concrete and normal fiber reinforced concrete) and strain-hardening behavior similar to many ductile metals (Li 1998, Li *et al* 2002). Strain-hardening response is accompanied by very large inelastic deformation, resulting in multiple tiny microcracks with widths of generally less than 100 μm. ECC also possesses compressive strength values similar to that of moderate-strength concrete with the range of 40–80 MPa and high-strength concrete with the strength values more than 80 MPa depending on mixture proportions, although the compressive strain capacity is nearly 50% higher.

As mentioned above, ECC is composed of ingredients similar to those used in conventional concrete and fiber reinforced concrete mixtures, meaning that under normal circumstances the material itself can be regarded as almost non-conductive. However, to achieve self-sensing ability, concrete-like material must be electrically conductive at a certain level. Over the years, naturally conductive materials such as iron-based aggregates, carbon nanotubes (CNTs), carbon black (CB), carbon fibers, graphite etc have been used to make it more conductive without sacrificing basic mechanical properties (Sanchez and Ince 2009, Baeza *et al* 2011, Tyson *et al* 2011a, Galao *et al* 2012). Several studies have also focused on re-engineering ECC mixtures with some of these naturally conductive materials to achieve self-sensing behavior (Hou and Lynch 2005, Lin *et al* 2011, Li *et al* 2013). Taking the relatively higher manufacturing costs of different conductive materials over conventional concrete ingredients into account, however, it is important to optimize conductive material dosage without compromising the highest possible electrical conductivity and basic mechanical properties. In this regard, the term 'electrical percolation threshold' can be defined as the minimum conductive material content over which sharp drops in the electrical resistivity (ER) of composite material start to be monitored, which is critical for self-sensing ability. Along these lines, an experimental study was undertaken to evaluate the electrical percolation thresholds of ECC matrices incorporating different electrically conductive carbon-based materials at nano- (multi-walled CNTs, graphene nanoplatelets (GNPs) and CB) and micro-scale (carbon fibers with 6 and 12 mm lengths (CF6 and CF12)). After deciding the percolation thresholds of electrically conductive materials in mortars through ER measurements, compressive strength measurements of mortars produced with the agreed-upon thresholds were recorded at 7, 28 and 90 d. ECC mixtures modified with the conductive materials were then produced and tested for self-sensing ability under uniaxial compressive loading after 7 and 28 d of initial curing. It is believed that incorporating a self-sensing attribute to ECC-like material, which has durability and mechanical properties that have already proven to be spectacular (Şahmaran and Li 2009), will multiply the benefits for sustainable civil infrastructures.

Table 1. Physical and chemical properties of PC, FA and silica sand.

Chemical composition, %	PC	FA	Silica sand
CaO	61.43	7.98	34.48
SiO_2	20.77	52.22	38.40
Al_2O_3	5.55	16.58	10.96
Fe_2O_3	3.35	6.60	0.81
MgO	2.49	2.10	7.14
SO_3	2.49	0.02	1.48
K_2O	0.77	1.53	0.86
Na_2O	0.19	0.86	0.18
Loss on ignition (LOI)	2.20	10.36	3.00
$SiO_2+Al_2O_3+Fe_2O_3$	29.37	75.40	50.17
Physical properties			
Specific gravity	3.06	2.10	2.60
Blaine fineness ($cm^2\ g^{-1}$)	3250	2690	—

2. Experimental program

2.1. Materials

ECC matrices were manufactured with general-use ordinary Portland cement (PC) similar to ASTM Type I, Class-F fly ash (FA), silica sand with maximum aggregate size of 0.4 mm, specific gravity of 2.6, water absorption capacity of 0.3%, drinkable mixing water and polycarboxylate ether based high range water reducing admixture (HRWRA) as common ingredients. Chemical and physical properties of PC, FA and silica sand are presented in table 1. Nano- and micro-scale conductive materials were used to make matrices electrically conductive for self-sensing tests. The nano-scale electrically conductive materials were multi-walled CNTs, GNPs and CB. CNTs were 20–30 nm in diameter, 10–30 μm in length, and with a surface area of more than 200 $m^2\ g^{-1}$. GNPs had a diameter of nearly 5 μm, thickness of 50–100 nm and surface area of nearly 13 $m^2\ g^{-1}$. The surface area and average particle size of CB were around 30–50 $m^2\ g^{-1}$ and 20–100 nm, respectively. The micro-scale electrically conductive materials used were chopped carbon fibers 6 and 12 mm long (CF6 and CF12), with aspect ratios of 800 and 1600, respectively. Both types of CF had tensile strength of 4200 MPa, elastic modulus of 240 GPa, elongation of 1.8%,

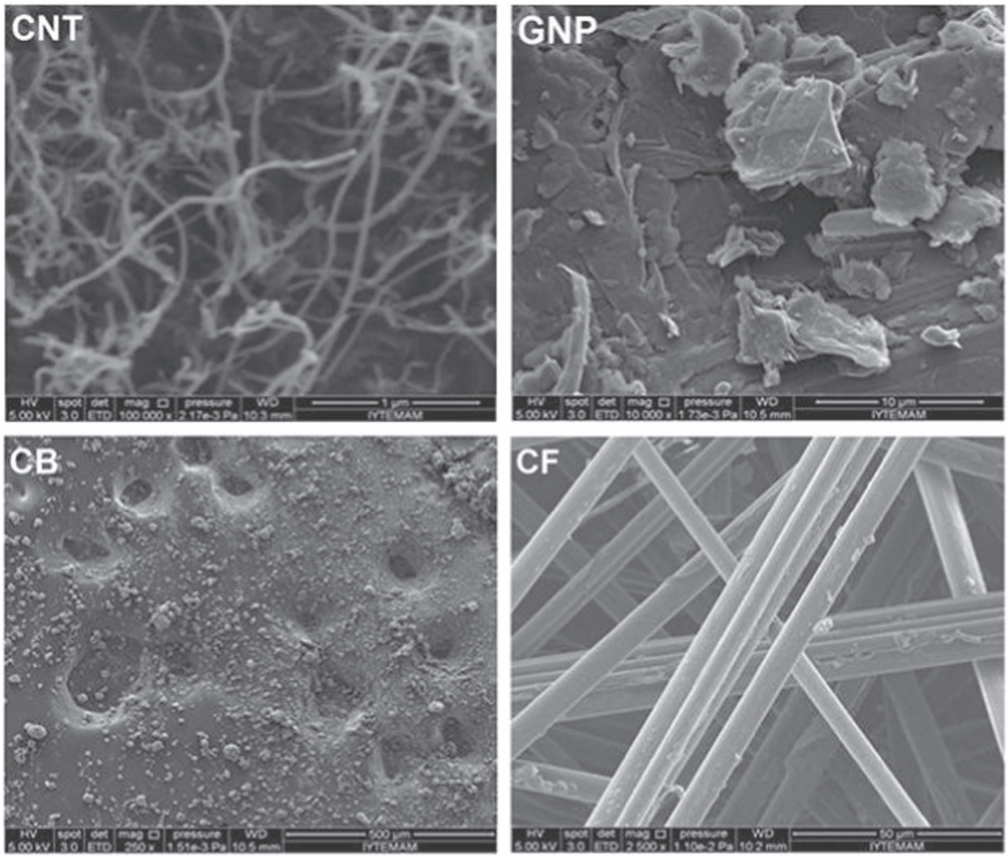

Figure 1. SEM photos of electrically conductive CNT, GNP, CB and CF.

density of nearly 1.7–2.0 g cm^{-3} and diameter of 7.5 μm. Scanning electron microscope (SEM) photos of CNT, GNP, CB and CF are shown in figure 1. To produce ECC mixtures for the self-sensing assessment, matrices incorporating different carbon-based conductive materials were reinforced with polyvinyl alcohol (PVA) fibers with a 39 μm diameter, 8 mm length, nominal tensile strength of 1620 MPa, elastic modulus of 42.8 GPa and specific gravity of 1.3. The utilization rate of PVA fibers was 2% by the total volume of the ECC mixture.

2.2. Proportioning and mixing

Both the matrix (without PVA fiber) and ECC (with PVA) mixtures in this study were produced with constant water to cementitious materials (CM = PC + FA) ratio (W/CM) of 0.27, and a FA/PC ratio of 1.2. Different dosages were used to specify the percolation thresholds of nano- and micro-scale carbon-based materials in mortar mixtures. Utilization rates of different carbon-based electrically conductive materials are shown in table 2. It must be noted that the dosages for carbon-based nano-scale materials (CNT, GNP and CB) were by the total weight of cementitious materials (PC + FA), while for micro-scale materials (CF6 and CF12), they were by the total volume of the mixture. Utilization rates for different carbon-based electrically conductive materials were selected based on previously conducted studies in the literature (Chen and Chung 1995, Xie *et al* 1996, Chen *et al* 2005, Coppola *et al* 2011, Gong *et al* 2011, Li *et al* 2011, Lin *et al* 2011, Sixuan 2012). As can be presumed, it was not possible to keep HRWRA amounts constant for all mixtures consisting of nano- and micro-scale carbon-based materials, which have relatively different particle sizes and specific surface areas. Mini slump flow spread tests were therefore performed to ensure similar workability characteristics in mixtures with relatively different compositions. During the tests, a truncated conical mold (with a diameter of 92 mm at the bottom, 44 mm at the top and a height of 76 mm) was placed on a smooth plate, filled with the mixture, then lifted upward. The slump flow deformation was defined as the dimension of the spread when the mixture stopped flowing (Khayat and Yahia 1998). Special care was taken to ensure that all mixtures reached similar flow deformation levels, with average mini slump flow diameters of approximately 160 mm.

According to previous studies, uniformly distributing conductive materials in cementitious systems is vital to creating a continuous electrical network that can capture or sense strain changes in real-life structures (Yazdanbakhsh *et al* 2011, Tyson *et al* 2011b, Sobolkina *et al* 2012). This concern was addressed in a recent paper of the authors, which proposed two different mixing methods for the highest electrical conductivity in cementitious composites, without sacrificing mechanical properties for both nano- and micro-scale carbon-based electrically conductive materials (Al-Dahawi *et al* 2016). Carbon-based materials were therefore made in accordance with that study. Accordingly, during the

Table 2. Utilization rates of carbon-based electrically conductive nano- and micro- scale materials.

Conductive material	Rate of conductive material utilization, %[a]																			
CNT	0.00	0.15	0.25	0.35	0.45	0.55	0.65	0.75	0.85	0.95	1.00	—	—	—	—	—	—	—	—	—
GNP	0.00	0.05	0.15	0.25	0.35	0.45	0.55	0.65	0.75	0.85	0.95	1.00	1.50	2.00	2.50	3.00	3.50	4.00	4.50	5.00
CB	0.00	1.00	2.00	3.00	4.00	5.00	—	—	—	—	—	—	—	—	—	—	—	—	—	—
CF	0.00	0.20	0.40	0.50	0.60	0.80	1.00	1.20	1.40	1.60	1.80	2.00	—	—	—	—	—	—	—	—

[a] By total amount of cementitious materials (PC + FA) for CNT, GNP and CB and total volume of mixtures for CF.

dispersion of electrically conductive carbon-based materials at nano-scale, CNT, GNP or CB was mixed with the entire amount of mixing water and HRWRA using a hand blender for 15 min at 3000 rpm. By the time this step was completed, the dry raw materials (PC, FA and silica sand) had been mixed for 10 min at 100 rpm in the mortar mixer. The previously prepared solution was then gradually added to the raw materials over 10 s and mixing continued for an additional 10 min at 300 rpm in a 5 l capacity mortar mixer. To uniformly disperse the micro-scale carbon-based materials (CF6 and CF12) in cementitious systems, CF6 or CF12 was first mixed with the dry raw materials (PC, FA and silica sand) in a 5 l capacity mortar mixer at 100 rpm for 10 min. After slowly adding the mixing water at 100 rpm over 10 s, speed was increased to 300 rpm, all of the HRWRA was added over 30 s, and mixing of all materials was continued for an additional 10 min at 300 rpm in the mortar mixer.

2.3. Specimen preparation and testing

To assess electrical percolation thresholds in different carbon-based materials, ER measurements of mortar specimens were recorded after 1, 7, 28, 60, 90 and 180 d. Cylindrical specimens measuring Ø100 × 200 mm were prepared for use in ER tests. After being kept in their molds at 50 ± 5% RH, 23 ± 2 °C for 24 h, specimens were removed and horizontally cut into four Ø100 × 80 mm pieces using two different Ø100 × 200 mm cylinders. This was done to prevent any possible disadvantages related to trowelled and/or molded surface conditions and to reduce the variations in ER measurements recorded from different pieces of a certain specimen. The cut-off specimens were then moved into isolated plastic bags to be cured until pre-determined testing ages at 95 ± 5% RH, 23 ± 2 °C. After finding the electrical percolation thresholds of matrix specimens in terms of ER results, 50 mm cubic ECC specimens from each mixture were produced, taking into consideration the previously determined thresholds for each carbon-based material. Three cubic specimens from each mixture were cured in a similar manner to that of the cylindrical specimens mentioned above, and tested for compressive strength after 7, 28 and 90 d of curing. The same number of reference specimens (without any carbon-based material) was cast for both ER and compressive strength testing, as well as for comparison of overall results. During the preparation of reference specimens, a mixing method similar to that used for specimens with CF was employed, but without CF.

A concrete resistivity meter with uniaxial configuration, which employs alternating current (AC) technique, was used in ER measurements. During ER testing, Ø100 × 80 mm pieces of cylindrical specimens were placed between two plate electrodes. Pre-wetted sponges (10 mm in height and 150 mm in diameter) were placed between the specimens and electrodes for adequate electrical contact. Sponges were pre-wetted with the same amount of water each time to prevent possible changes in electrical measurements. Individual ER measurements of pre-wetted sponges were performed and no associated results were obtained, thus the ER measurements of cylindrical specimens were used without modifying the values due to the ER of sponges. The concrete resistivity meter used included frequency options ranging from 1 to 30 kHz. However, the working frequency during ER testing was set at 1 kHz, based on a suggestion made by (Hou 2008), which stated that when AC current is applied, polarization effect can be avoided with a working frequency of at least 1 kHz. With the completion of ER testing, the concrete resistivity meter showed impedance and corresponding phase angle values (between 0°–180°), which were used to obtain final resistivity results with the help of geometrical factors. To calculate the ER results using impedance, phase angle and geometrical factors, the following equation was used:

$$\rho = Z \times \cos(\theta) \times \frac{A}{L},$$

where, ρ, Z, θ, A and L stand for resistivity (Ω m), electrical impedance (Ω), phase angle (°), cross-sectional area (m^2) and length (m) of the specimen, respectively.

To determine self-sensing ability, ECC mixtures with nano- and micro-scale carbon-based conductive materials were produced, taking different percolation thresholds into account. The reason for using ECC specimens rather than matrices (without PVA fibers) to capture changes in electrical measurements with applied stress was to observe self-sensing of damage at very large deformation levels. As stated previously, self-sensing ability was measured under uniaxial compressive loading, and a special testing configuration was proposed for this purpose using 50 mm cubic specimens similar to those used for compressive strength evaluation. To prevent the possible effects and variations of internal moisture on ER results under compressive loading, 7 and 28 d old cubic ECC specimens with and without (reference) electrically conductive materials to be tested for self-sensing were dried in an oven at 60 °C for 24 h starting on the 6th and 27th d, respectively. To record the electrical measurements from the specimens directly, electrically conductive materials embedded inside the matrices of ECC specimens were used as electrodes. Although different electrode types such as steel mesh, copper mesh and wire, brass plate, aluminum foil etc were used, due to the ease of embeddability and more reasonable sensing results, brass plates were used in this study (figure 2(a)). The proposed electrode configuration is shown schematically in figure 2(b). As seen from this figure, two 10 × 60 mm (width × length) brass plate electrodes were embedded parallel to each other inside a 50 mm cubic specimen during the fresh state (two-point probing). Electrodes were inserted 5 mm inward from the opposite faces of cubic specimens and very close to the top surface. Before actual electrode configuration was selected, brass electrodes were tested in different sizes and locations. The configuration selected offered the most reasonable results with the greatest accuracy. The tests were implemented with great care, and in order for ER testing to be more sensitive, insulating plastic covers were inserted between the specimens and compressive loading plates to interrupt any possible electrical contact for each time of measurement (figures 2(c) and (d)). Given that the insulating covers used to cut the electrical contact might

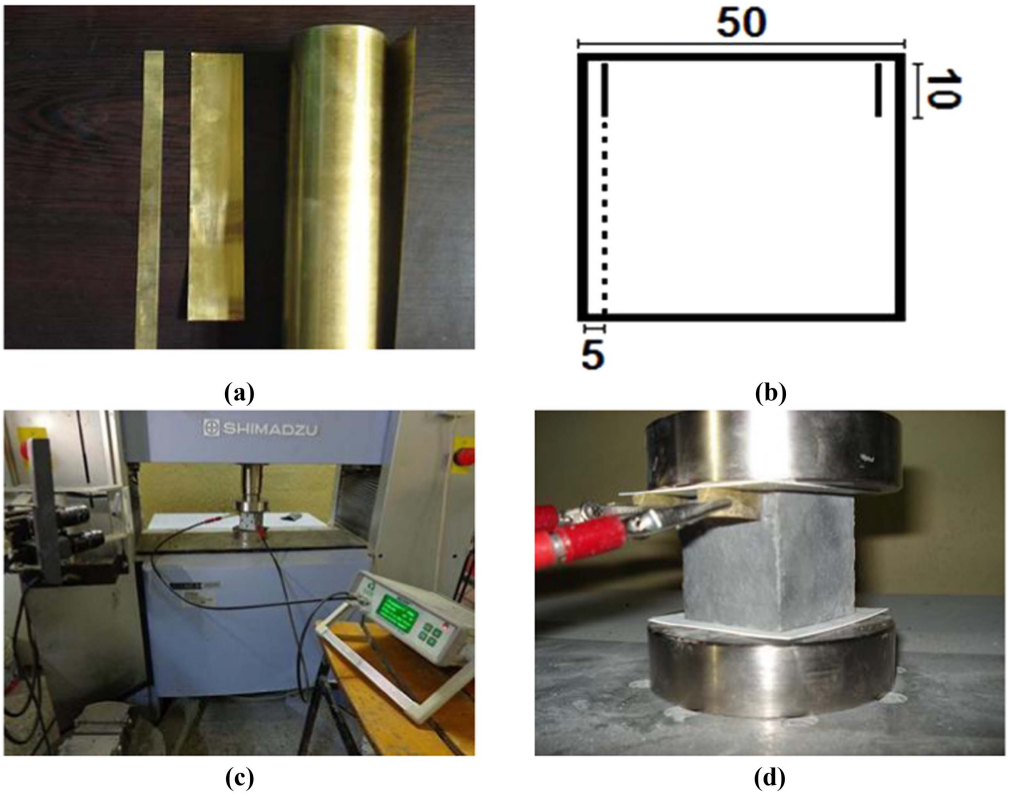

Figure 2. (a) Brass plate that was used as embedded electrodes during self-sensing tests (b) proposed configuration for self-sensing test (units are in mm) (c) testing of cubic specimens for self-sensing of strain (d) a closer view of specimen taken during testing.

affect deformation levels in compression, a video extensometer was used to record deformation values during compressive testing, and the values were average, in addition to using results taken directly from the loading device itself. Electrical measurements from the concrete resistivity meter were recorded every five seconds and the values were plotted against the average deformation values in compression to evaluate self-sensing ability of different ECC mixtures. Since the brass electrodes were further separated with increments in compressive loading, ER results were expected to increase as well.

3. Results and discussion

3.1. Electrical resistivity

3.1.1. Matrix specimens with nano-scale carbon-based materials. Average ER results of matrix specimens produced with different nano-scale electrically conductive carbon-based materials (CNT, GNP and CB) are shown as raw data in table 3 and as a graphical illustration in figure 3 for clearer understanding. The values were obtained at the end of 1, 7, 28, 60, 90 and 180 d of initial curing from four Ø100 × 80 mm mortar cylinders.

ER test results of all matrix specimens showed an increasing trend with prolonged curing age (table 3). Taking the average ER results of CNT-0.05 mortar mixtures as an example, while 1 d results were 5.64 Ω m, values were 16.75, 57.80, 188.57, 241.61, 601.56 Ω m after 7, 28, 60, 90 and 180 d of initial curing, respectively. This trend was observable for all tested specimens, regardless of the type of carbon-based electrically conductive material used. These results are in line with the literature (Liu *et al* 2013). As seen from table 3, increments in results with time became more dramatic at longer curing ages. This was attributed to ongoing hydration and further pozzolanic capability influencing the porosity, pore solution chemistry and tortuosity of the pore network, which have been reported to be the main parameters in relation to ER (Spragg *et al* 2013, Yıldırım *et al* 2015). Moreover, in addition to their effect on pore characteristics, final hydration products such as C–S–H gels and CH are likely to cause abrupt increments in ER results by surrounding and/or disconnecting the conductive materials, especially for specimens produced with conductive materials (Liu *et al* 2013).

Although the extent of their effectiveness differed, all nano-scale carbon-based materials proposed in this study were more effective in lowering ER results of mortar specimens than control mixtures at the end of each initial curing age. This is clearly illustrated in the ER results presented in figure 3, which show that sharp reductions in ER values of mortar specimens took place even with slight utilization rates of nano-scale carbon-based materials. This outcome was expected, given the relatively high specific surface areas and electrical conductivity of CNT, GNP and CB. Figure 3 also shows differences in the performance of different nano-scale carbon-based materials in decreasing ER.

Table 3. ER measurements of mortar specimens incorporating nano-scale electrically conductive carbon-based materials (units are in Ω m).

Mixture ID.	Rate of conductive material, %	1 d	7 d	28 d	60 d	90 d	180 d
Control	0.00	9.67	20.92	90.65	330.00	620.22	1252.23
CNT-0.05	0.05	5.64	16.75	57.80	188.57	241.61	601.56
CNT-0.15	0.15	4.97	14.78	51.17	157.14	238.66	597.14
CNT-0.25	0.25	4.15	13.01	46.11	141.92	223.44	518.57
CNT-0.35	0.35	3.59	12.95	43.12	128.66	219.51	484.69
CNT-0.45	0.45	2.94	12.87	38.21	115.89	207.23	468.97
CNT-0.55	0.55	2.87	11.79	33.93	113.44	190.04	417.90
CNT-0.65	0.65	2.06	10.70	33.17	103.13	178.75	374.20
CNT-0.75	0.75	1.57	9.70	30.08	102.83	164.02	362.41
CNT-0.85	0.85	1.42	9.30	28.24	75.97	137.50	339.82
CNT-0.95	0.95	1.37	8.72	24.01	64.13	117.86	312.81
CNT-1.00	1.00	1.20	8.23	22.25	58.19	102.14	276.47
GNP-0.05	0.05	6.83	18.02	67.08	145.85	245.04	637.90
GNP-0.15	0.15	6.81	17.53	64.23	143.88	242.10	633.48
GNP-0.25	0.25	6.77	17.51	62.32	141.43	238.17	625.13
GNP-0.35	0.35	6.62	17.47	61.43	140.94	234.24	624.64
GNP-0.45	0.45	6.41	17.21	59.76	136.52	228.84	607.95
GNP-0.55	0.55	6.35	15.96	53.82	135.04	226.38	580.94
GNP-0.65	0.65	6.23	15.03	53.74	133.57	220.98	576.03
GNP-0.75	0.75	6.20	14.91	53.49	133.57	219.02	564.24
GNP-0.85	0.85	6.12	14.83	52.97	131.61	218.04	546.56
GNP-0.95	0.95	6.02	14.79	52.88	124.24	216.07	522.01
GNP-1.00	1.00	5.98	14.78	52.84	121.29	216.07	518.57
GNP-1.50	1.50	5.97	14.00	40.02	120.80	187.10	514.64
GNP-2.00	2.00	5.85	13.41	41.10	119.33	182.68	501.88
GNP-2.50	2.50	5.84	13.38	40.32	110.00	175.80	447.86
GNP-3.00	3.00	5.52	13.33	39.14	98.61	161.07	399.24
GNP-3.50	3.50	5.52	13.31	36.39	97.53	160.09	396.29
GNP-4.00	4.00	4.80	12.72	34.72	95.42	158.13	390.89
GNP-4.50	4.50	4.72	12.23	34.21	88.29	143.88	356.03
GNP-5.00	5.00	4.13	12.52	33.89	86.58	139.96	338.84
CB-1.00	1.00	6.91	20.33	56.18	131.61	242.10	635.45
CB-2.00	2.00	5.39	17.29	50.83	125.71	227.37	607.95
CB-3.00	3.00	5.40	17.04	49.79	124.73	210.18	545.09
CB-4.00	4.00	3.81	16.70	47.09	118.84	197.90	442.95
CB-5.00	5.00	3.42	15.22	42.48	104.11	188.57	359.46

At the end of all initial curing ages, specimens produced with CNT showed sharper reductions in ER values than those with GNP and CB. However, to be more precise, it is more logical to compare the results recorded from matrices incorporating the same level of nano-scale conductive materials. The only conductive material rate simultaneously used for all mixtures with CNT, GNP and CB was 1%. Based on the ER results of 28 d old CNT-1.00, GNP-1.00 and CB-1.00 mixtures, average electrical conductivity of specimens increased by 76%, 42% and 38%, respectively, in comparison to control specimens of the same age. Additionally, the superior performance of CNT was valid for all pre-set initial curing ages. As detailed in the previous sections, CNT particles have substantially higher specific surface areas (more than 200 $m^2 g^{-1}$) than GNP (~13 $m^2 g^{-1}$) and CB (~30–50 $m^2 g^{-1}$), which increases the chance for CNT-bearing matrices to result in higher ER values by filling the spaces among hydration products and lowering overall porosity. Furthermore, CNT particles are at the diameters close to C–S–H gel layers, and are therefore wrapped by C-S-H gels when included in a cement-based matrix (Makar and Beaudoin 2004, Gengying and Peiming 2005, Raki *et al* 2010). According to some researchers, this interrupts the contact between the CNT bundles, causing lower electrical conductivity (Raki *et al* 2010). The current study, however, showed that with a mixing method capable of uniformly distributing the CNT particles, electrical conductivity can be improved significantly despite the possibility of CNT particles being wrapped by hydration products (Al-Dahawi *et al* 2016). Uniform distribution of CNT in cementitious matrices appears to have led individual particles to bridge cracks and voids in the microstructure, guaranteeing higher electrical conductivity, as shown in table 3.

One of the important points regarding the data presented in table 3 and figure 3 is that despite continuous reductions in ER measurements of all types of specimens produced with

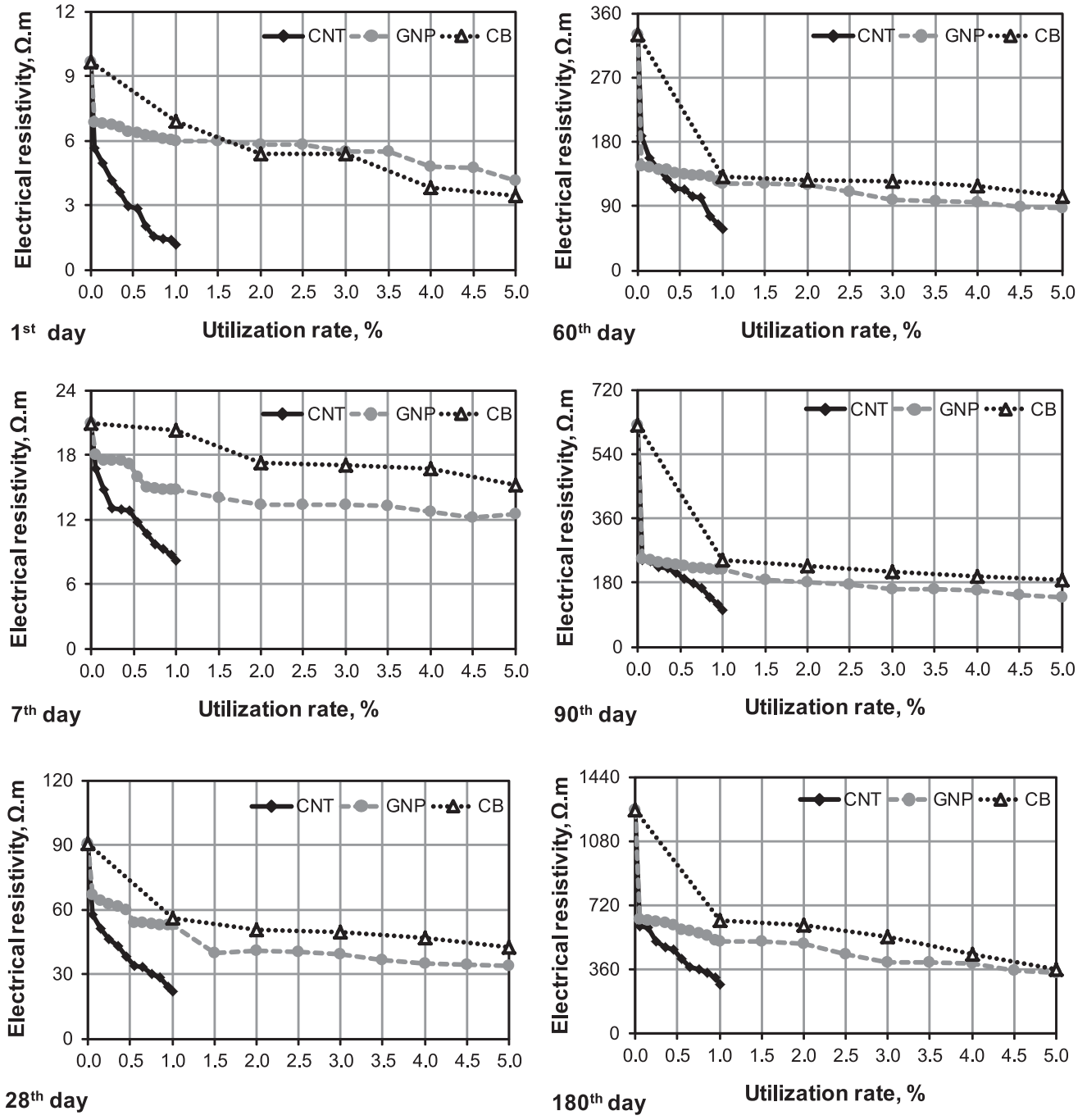

Figure 3. Changes in the ER results of mortar specimens produced with different rates of nano-scale electrically conductive carbon-based materials.

different nano-scale carbon-based conductive materials, the rate of reductions was not explicit from a certain point, implying saturation of cementitious matrices with nano-scale carbon-based materials. This leads to a 'percolation threshold,' which is a zone rather than a single content of conductive material, resulting in sudden escalations in electrical conductivity (Li *et al* 2006). Percolation thresholds of mortar specimens produced with different nano-scale carbon-based materials are more visible in figure 3. The figure shows that regardless of changes in initial curing age, percolation thresholds did not change for mortar specimens with different nano-scale carbon-based conductive materials. Percolation thresholds for the CNT-, GNP- and CB-incorporated mixtures were around 0.55%, 2.00% and 2.00%, respectively; at utilization rates above this limit, there were no significant reductions in ER values. The changes in ER results of control specimens with maximum utilization rates and the highest use of percolation thresholds show this clearly. Using CNT-bearing specimens as an example, with the highest utilization rate of 1.00%, the average 1 d ER result of control specimens decreased by 88% (from 9.67 to 1.20 Ω m). When the percolation threshold (0.55%) was

Table 4. ER measurements of mortar specimens incorporating micro-scale electrically conductive carbon-based materials (units are in Ω m).

Mixture ID.	Rate of conductive material, %	1 d	7 d	28 d	60 d	90 d	180 d
Control	0.00	9.67	20.92	90.65	330.00	620.22	1252.23
CF6-0.20	0.20	7.07	14.24	44.05	117.37	216.56	418.63
CF6-0.40	0.40	6.72	13.40	37.25	109.02	209.20	367.32
CF6-0.50	0.50	5.96	12.77	32.31	67.03	123.40	200.19
CF6-0.60	0.60	4.32	9.06	19.05	40.37	44.00	108.94
CF6-0.80	0.80	3.55	6.89	13.41	27.60	36.88	69.89
CF6-1.00	1.00	3.01	6.26	11.69	23.23	23.87	56.28
CF6-1.20	1.20	2.90	5.95	12.57	16.65	23.87	38.65
CF6-1.40	1.40	2.58	4.84	11.98	14.73	21.56	33.24
CF6-1.60	1.60	2.68	5.68	11.64	15.17	20.92	36.03
CF6-1.80	1.80	2.46	5.26	9.79	14.39	16.40	25.64
CF6-2.00	2.00	2.58	5.90	11.44	12.13	15.52	31.10
CF12-0.20	0.20	6.67	12.23	32.41	97.63	182.58	338.40
CF12-0.40	0.40	5.61	11.39	27.99	69.04	121.15	223.47
CF12-0.50	0.50	5.05	10.75	24.21	55.34	95.56	186.92
CF12-0.60	0.60	4.14	9.05	18.22	42.97	67.28	131.23
CF12-0.80	0.80	3.45	7.92	16.21	34.67	51.71	103.79
CF12-1.00	1.00	2.71	5.68	10.73	20.43	30.64	61.16
CF12-1.20	1.20	2.25	5.56	10.41	15.62	30.45	35.10
CF12-1.40	1.40	1.97	4.95	8.91	12.65	24.31	28.64
CF12-1.60	1.60	2.32	5.98	11.39	16.94	22.59	27.40
CF12-1.80	1.80	2.12	5.70	12.38	19.74	18.91	21.12
CF12-2.00	2.00	1.86	5.25	7.60	10.05	13.01	13.54

selected, on the other hand, the same ER results decreased by 70% (from 9.67 to 2.87 Ω m). These findings demonstrate that 70% of the electrical conductivity had already been achieved when almost half of the highest CNT utilization rate amount was selected in the matrices. In other words, specimens became saturated to CNT inclusion after the electrical percolation threshold. The same behavior occurred in specimens with GNP and CB, although higher quantities (2.00%) were needed to make the corresponding matrix specimens saturated for high electrical conductivity than with CNT utilization.

Another interesting point related to figure 3 is that there were more obvious decrements in ER measurements of CNT-incorporated specimens, even beyond the percolation threshold, than in GNP- and CB-incorporated specimens. This shows the superior capability of CNT particles over GNP and CBs in enhancing the electrical properties of cementitious materials, as long as uniform dispersion is guaranteed. The final recorded percolation thresholds for mortar mixtures with CNT (0.55%), GNP (2.00%) and CB (2.00%) were close to or lower than those reported in the literature (Coppola *et al* 2011, Gong *et al* 2011, Li *et al* 2011, Sixuan 2012).

3.1.2. Matrix specimens with micro-scale carbon-based materials. Table 4 displays raw ER data for matrix specimens incorporating different rates of micro-scale electrically conductive carbon-based materials (CF6 and CF12) after 1, 7, 28, 60, 90 and 180 d of initial curing. The same results are shown in graphical form in figure 4. Table 4 presents the average results from four Ø100 × 80 mm mortars. Like CNT-, GNP- and CB-bearing specimens, ER results of specimens produced with CF6 and CF12 also increased when initial curing age was extended; possible causes have been explained above.

Like nano-scale carbon-based electrically conductive materials, CFs were very influential in lowering the ER results of control specimens. For example, with a utilization rate of only 0.20%, the average ER result of the 180 d old control specimen decreased from 1252.23 Ω m to 418.63 Ω m and 338.40 Ω m for CF6 and CF12; showing 67% and 73% percentage decrements, respectively. The same behavior also occurred in other specimens at different ages. Using longer CF12 caused lower ER results than CF6 at the end of all initial curing ages. In specimens with longer CFs, this behavior was in line with what has been previously stated in the literature (Chen *et al* 2004, Al-Dahawi *et al* 2016). It can be attributed to the higher probability of longer CFs providing more continuous electrically conductive paths by favoring contact among individual fibers along the whole length of each tested specimen. Although including CF caused constant reductions in ER results, this behavior was much more evident at certain CF utilization levels, regardless of the selected length, which highlights the saturation of specimens with these materials. Figure 4 shows that sudden changes in the ER of specimens with both CF6 and CF12 took place at a percolation threshold of 1.00% for all testing ages. This result is line with Chen and Chung (1995).

When ER results recorded from mortars produced with nano- (CNT, GNP and CB) and micro-scale (CF6 and CF12) electrically conductive carbon-based materials are compared, specimens with CF12 showed minimum values, followed by specimens with CF6, CNT, GNP and CB. This behavior of

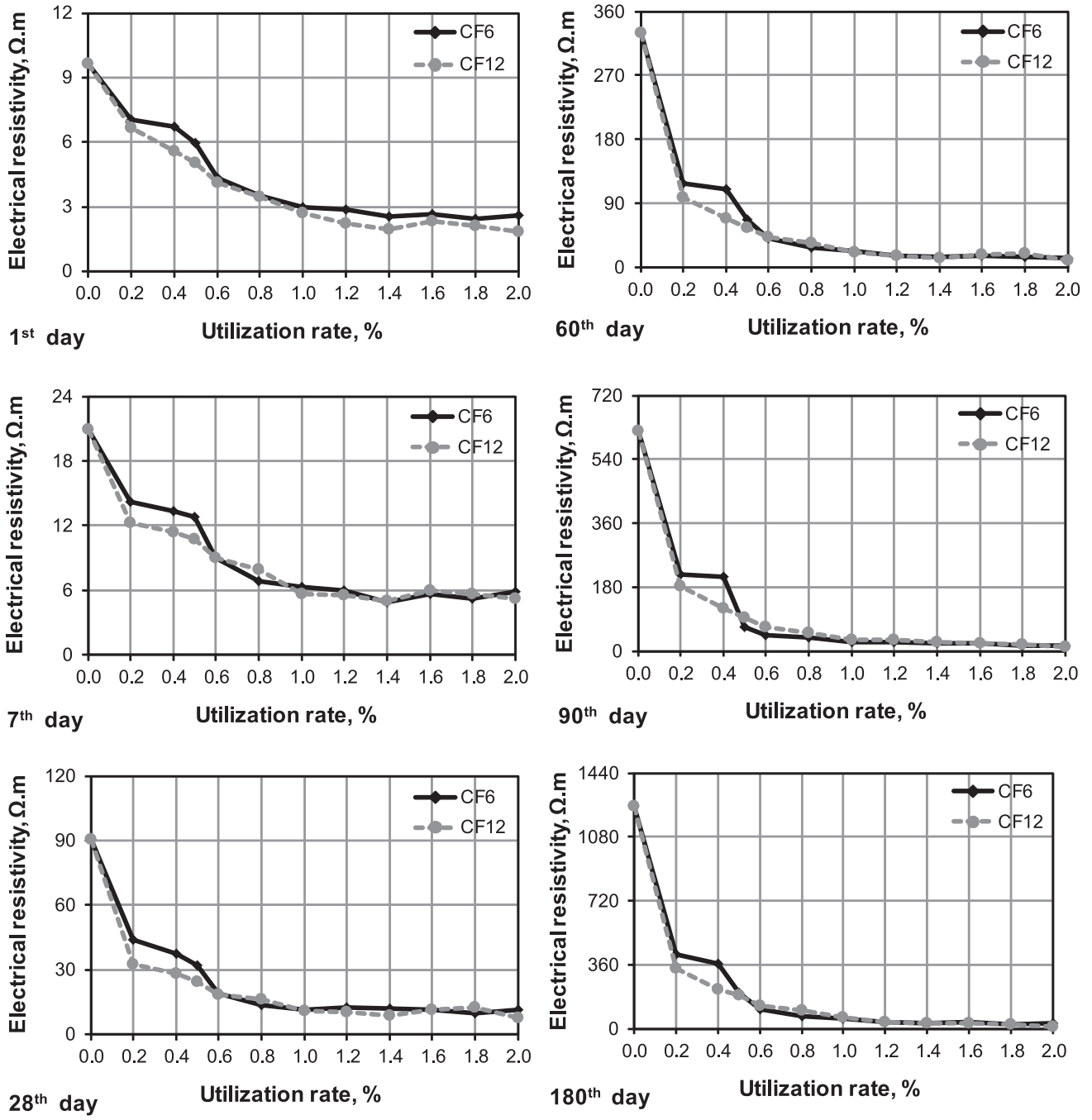

Figure 4. Changes in the ER results of mortar specimens produced with different rates of micro-scale electrically conductive carbon-based materials.

CF12 specimens was more pronounced at later ages, which can be seen in figure 4. The figure shows that ER results of CF-bearing specimens decreased drastically, especially at later ages, approaching levels close to zero, unlike specimens with CNT, GNP and CB (figure 3). Taking the lower production cost of CF over CNT, GNP and CB, CF appears to provide better electrical properties than CNT, GNP and CB, without necessitating a complicated, time-consuming mixing method. Moreover, it has been reported that CFs contribute to mechanical properties such as flexural strength, flexural toughness, tensile strength and ductility and reduced drying shrinkage (Wen and Chung 2007). On the other hand, Wen and Chung (1999) stated that piezoresistivity (the dependence of ER on applied strain) of CF-based cementitious composites is irreversible since the CFs break when strain levels greater than 0.2% are reached. This makes cementitious composites produced with CF unsuitable for detecting strain and/or stress changes in heavily strained conditions. On the contrary piezoresistive characteristics of CNT particles are highly reversible, even under strain levels as high as 3.4%, which makes cementitious composites reinforced with CNTs a promising material for sensing in heavily strained conditions

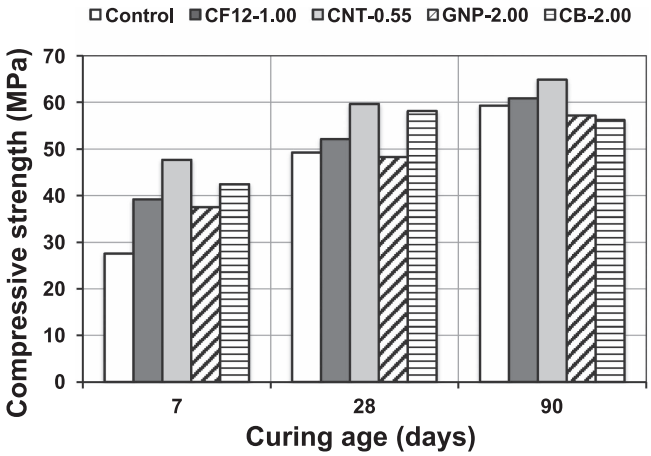

Figure 5. Compressive strength results of mortar specimens produced with different carbon-based electrically conductive materials.

(Tombler *et al* 2000). Based on the findings of the current study and suggestions made by researchers in literature, therefore, using CFs or CNTs seems to be more beneficial, depending on the self-sensing need of cementitious composites, due to their superior electrical and mechanical properties (discussed in the next section).

3.2. Compressive strength

Compressive strength test results of mortar specimens are outlined in figure 5, which shows the average compressive strength results of six 50 mm cubic specimens at the end of 7, 28 and 90 d of initial curing. The results are for specimens produced with different nano- and micro-scale carbon-based materials, using the previously explained percolation thresholds. Results for specimens with CF6 have not been included in this figure, since specimens with CF12 had higher compressive strength results (Al-Dahawi *et al* 2016).

Based on the data in figure 5, compressive strength results showed an incremental trend regardless of carbon-based material. For example, the average 7, 28 and 90 d compressive strength results of CF12-1.00 mortar specimens were 39.2, 52.1, 60.8 MPa, respectively. Despite increases in compressive strength with further curing, however, the increments were more pronounced in control specimens than in those with carbon-based materials. This was especially evident in specimens with nano-scale carbon-based materials. For instance, the increment rate in the compressive strength results of control specimens between 7 and 90 ds was (116% —from 27.5 to 59.3 MPa), while the same values were 55% (from 39.2 to 60.8 MPa), 36% (from 47.7 to 64.8 MPa), 52% (from 37.5 to 57.1 MPa) and 32% (from 42.4 to 56.2 MPa) for specimens with CF12, CNT, GNP and CB, respectively. This may be because of the availability of higher number of nucleation sites at earlier ages in the case of CNT-, GNP-, and CB-bearing specimens, as mentioned below, which permits to gain high earlier compressive strength with low rate of increment at the later ages. The less pronounced increments in compressive strength with further curing of nano-scale carbon-based materials can also be attributed to the fact that the matrices of specimens with CNT, GNP, and CB were highly packed due to the substantially high specific surface areas of these materials, which led to less available space for newly formed hydration products to settle, contributing to strength development.

In looking at the changes in compressive strength results of specimens with different carbon-based electrically conductive materials, figure 5 shows that CNT-0.55 matrix specimens exhibited the highest values at the end of each predetermined testing age. This finding correlates with the lower ER results recorded from specimens with CNT compared to those with GNP and CB. Higher compressive strength results noted from specimens incorporating CNT were attributed to the higher specific surface areas of CNT particles, which provided more nucleation sites, stronger packing through densification of matrices with filler effect, improved particle size distribution and flaw-bridging effect at nano-scale. Since higher compressive strength results are generally associated with lower overall porosity, disconnected pores, lower amounts of pore solution, etc, higher ER results might be expected from these specimens. However, it is important to note that with a suitable mixing method for uniform distribution of nano-scale carbon-based materials, the possible effects of the abovementioned parameters on increasing ER results can be counteracted by taking advantage of the superior electrical characteristics of such materials. Compared to control specimens, there were also increments in the compressive strength results of specimens at different ages after including CF12, due to the capability of CF12 to arrest crack growth. CF12 fibers are likely to act as internal pore and/or microcrack bridging reinforcements, which are also effective in modifying pre- and post-peak microcracking behavior and resulting in higher compressive strength results than control specimens. Although ER results of CF12-bearing specimens were the lowest, compressive strength results were not generally as high, possibly due to the fact CFs are at micron levels and do not have a significant impact on particle packing and improved gradation.

3.3. Self-sensing behavior under compressive loading

50 mm cubic ECC specimens were manufactured to evaluate self-sensing ability under compressive loading. In addition to control specimens with no carbon-based electrically conductive materials, ECCs incorporating CF12, CNT, GNP and CB were also produced for self-sensing purposes. The utilization rates of different micro- and nano-scale conductive materials for ECC production were selected based on the previously determined percolation thresholds (0.55%, 2.00%, 2.00% and 1.00% for CNT, GNP, CB and CF12, respectively). ECC mixtures with CF6 were not used since the electrical properties of ECC matrices with CF12 were better, as described in previous sections. Tests were carried out based on changes in ER of ECC specimens recorded from two separate embedded brass electrodes, as explained earlier. Three 7 and 28 d old cubic specimens from each mixture were tested and average results were taken into consideration.

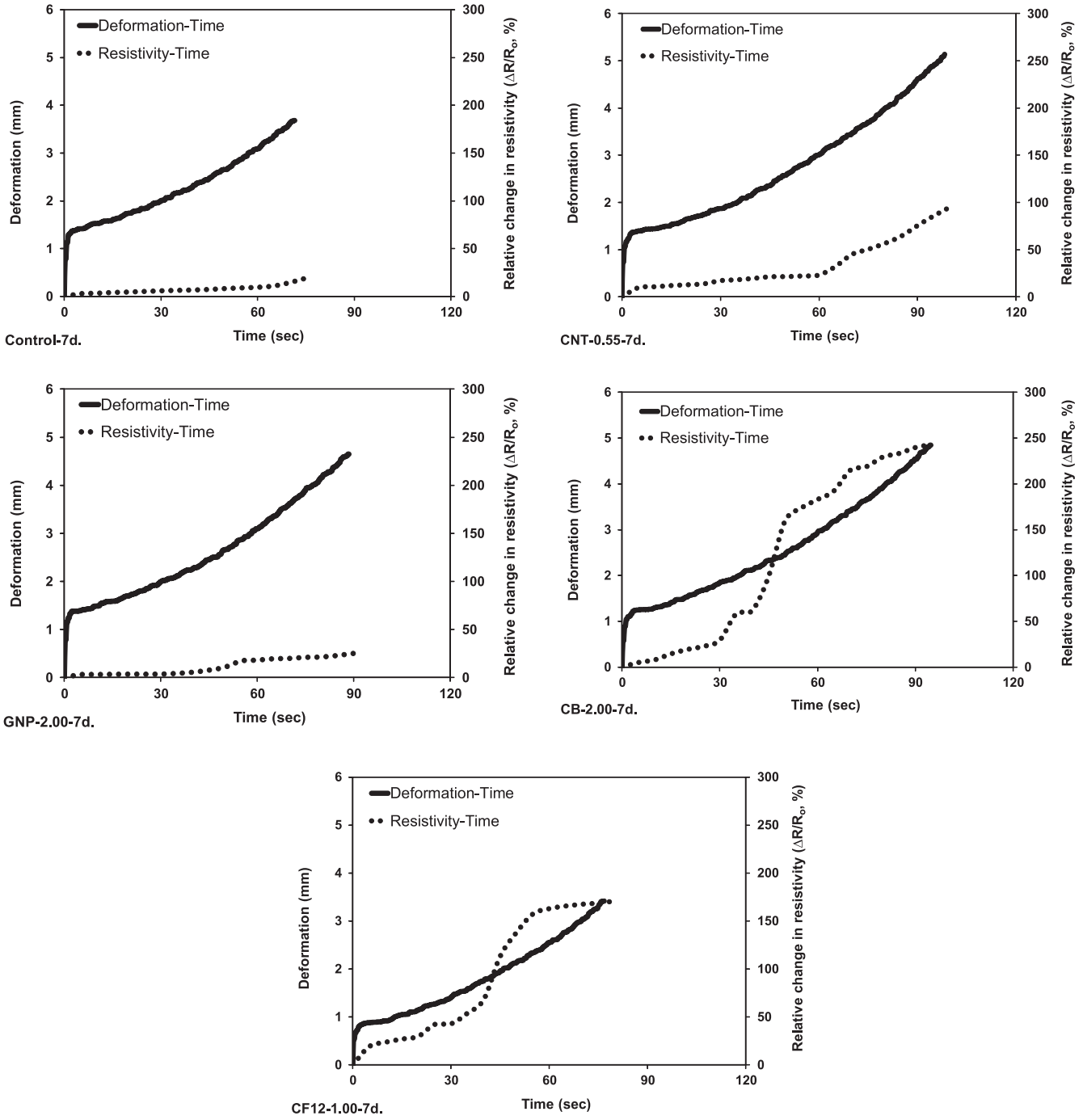

Figure 6. Mechanical and electrical behavior of 7 d old ECC specimens with and without carbon-based conductive materials under compressive loading.

Percentage changes in ER measurements of different ECC specimens relative to bulk ER (without any loading) ($\Delta R/R_0$) and deformation in compression (mm) were plotted against testing time. Figures 6 and 7 show results for specimens initially cured for 7 and 28 d, respectively.

The two figures clearly demonstrate that application of compressive loading caused ER results of control ECC specimens to increase, as expected, due to brass electrodes being separated from each other. This behavior was irrespective of initial curing age, although it was slightly more pronounced for 7 d old specimens, most probably due to higher amounts of internal water. Control ECC specimens without additional carbon-based material were responsive to deformation from the beginning of loading due to the high unburned carbon content (LOI) of class-F FA used during specimen production. It should be noted that even without complex modifications to the chemical composition, ECC control mixtures were favorable for the self-sensing of mechanical damage, especially at early ages of hydration. However, large deformation levels were necessary for this behavior to occur.

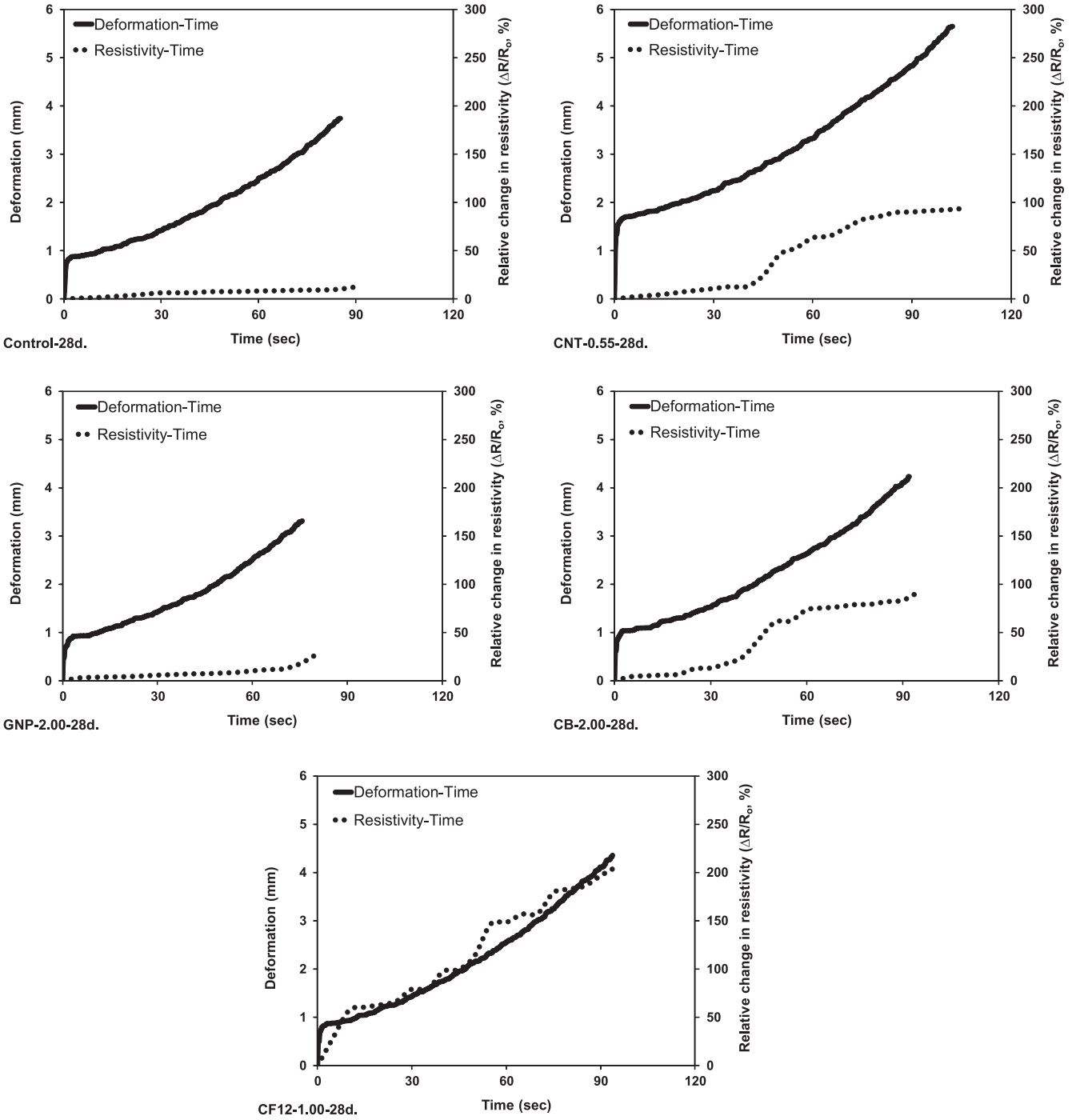

Figure 7. Mechanical and electrical behavior of 28 d old ECC specimens with and without carbon-based conductive materials under compressive loading.

Although the extent of deformation varied depending on the selected material, use of different carbon-based electrically conductive materials significantly modified the deformation-sensing properties of specimens, which can be seen in figures 6 and 7. Regardless of initial aging and the carbon-based material used, self-sensing capability was valid for all mixtures. Among all the carbon-based materials, GNPs were the least effective in terms of self-sensing performance, although they resulted in better performance (higher percentage changes in $\Delta R/R_0$) than the control specimens at 7 and 28 d. GNPs were followed by CNT particles in terms of self-sensing performance. Although CNT-bearing specimens sensed deformation in compression starting from initial loading, the behavior was much more evident after a certain deformation level (mid-range) for both initial curing ages, as indicated in figures 6 and 7. Although the self-sensing performance of CB and CF12 materials was comparable, CF12 exhibited the best performance. Figures 6 and 7 show that ECC specimens with CF12 were able to sense even relatively small deformation levels, starting at the beginning of loading,

regardless of initial curing age. CB-bearing ECC specimens behaved similarly, although self-sensing behavior was more pronounced for younger specimens. As reported, CNT, CB and CF12 utilization seems more advantageous for self-sensing purposes, with the best performance obtained from specimens with CF12. However, factors such as individual electrical properties of the material, necessity of elaborate mixing methods for uniform dispersion, manufacturing cost, reasonable mechanical properties and so on should also be taken into consideration.

Figures 6 and 7 also show that the changes in relative ER results were slightly smoother at the very beginning of compressive loading and became more pronounced after a certain level due to the changes in crack characteristics of ECC specimens upon compressive loading. At the initial stages of compressive loading, changes in ER were generally less pronounced, since very few or no microcracks formed during this period. With the further increment of compressive loading (plastic stage), escalations in ER started to take place, since microcracks (which are physical barriers against the movement of electrically conductive ions and/or agents) started to form. Upon further loading (around the stage of failure), abrupt increments in ER results were visible for almost all ECC specimens of different ages. Although ECC specimens exhibited multiple microcracking, failure occurred when one of the microcracks started to localize. Based on this finding, it can be stated that localization of a single microcrack leads to sudden changes in ER results, and not multiple microcrack formation. This result is line with the study conducted by Yıldırım *et al* (2015), who concluded that crack width is more decisive on the electrical properties of ECC specimens than crack number.

4. Conclusions

A detailed study was undertaken to determine the electrical percolation thresholds of different carbon-based nano- (CNT, GNP and CB) and micro-scale (CF6 and CF12) materials in cementitious materials, using ER measurements of ECC matrix specimens. After determining electrical percolation thresholds, compressive strength tests were performed on ECC mortars. As a final step, self-sensing of damage created under compressive loading was assessed on ECC specimens with and without carbon-based materials. The following conclusions were reached:

- Incorporating different carbon-based nano- and micro-scale electrically conductive materials into the cementitious systems of ECC mortars resulted in substantially lower ER results compared to control specimens, regardless of pre-set initial curing ages, although there were certain utilization rates above which no significant drops in ER were evident (electrical percolation thresholds). Irrespective of initial curing age, electrical percolation thresholds of CNT, GNP, CB and CFs (both CF6 and CF12) were 0.55%, 2.00%, 2.00% and 1.00%, respectively, based on the proposed utilization rates.
- Compared to control specimens, there were considerable improvements in the compressive strength measurements of mortar specimens when different carbon-based materials were incorporated at the rate of percolation threshold, irrespective of initial curing age. Even the lowest compressive strength attained at the end of 7 d (from GNP-2.00 specimens with 37.5 MPa) was more than adequate for many civil engineering applications.
- Piezoresistive properties of ECC specimens produced with and without electrically conductive carbon-based materials in the presence of compressive loading were confirmed, although this result was more pronounced for younger specimens with conductive materials. Although bulk ER results of mortar specimens reinforced with CNT and CF12 particles were lower than those of other conductive materials, all the carbon-based materials, especially CNT, CB and CF12, proved themselves worthy in capturing changes in compressive damage.
- Although all selected carbon-based materials were effective in enhancing the electrical, mechanical and self-sensing properties of cementitious composites, CNTs and CFs seemed to contribute more to these properties overall. However, due to the differences in production costs, ease of uniform dispersability, etc the selection should be made with care, depending on the self-sensing need.

Acknowledgments

The authors gratefully acknowledge the financial assistance of the Scientific and Technical Research Council (TUBITAK) of Turkey provided under Project: 114R043.

References

Al-Dahawi A, Öztürk O, Emami F, Yıldırım G and Şahmaran M 2016 Effect of mixing methods on the electrical properties of cementitious composites incorporating different carbon-based materials *Constr. Build. Mater.* **104** 160–8

Baeza F J, Galao O, Zornoza E and Garces P 2013 Multifunctional cement composites strain and damage sensors applied on reinforced concrete (RC) and structural elements *Materials* **6** 841–55

Baeza F J, Zornoza E, Andion L G, Ivorra S and Garces P 2011 Variables affecting strain sensing function in cementitious composites with carbon fibers *Comput. Concr.* **8** 229–41

Chen B, Liu J and Wu K 2005 Electrical responses of carbon fiber reinforced cementitious composites to monotonic and cyclic loading *Cem. Concr. Res.* **35** 2183–91

Chen B, Wu K and Yao W 2004 Conductivity of carbon fiber reinforced cement-based composites *Cem. Concr. Compos.* **26** 291–7

Chen P W and Chung D D L 1995 Improving the electrical conductivity of composites comprised of short conducting fibers in a nonconducting matrix: the addition of a nonconducting particulate filler *J. Electron. Mater.* **24** 47–51

Chung D D L 2002 Electrical conduction behaviour of cement-matrix composites *J. Mater. Eng. Perform.* **11** 194–204
Chung D D L 2003 Damage in cement-based materials, studied by electrical resistance measurement *Mater. Sci. Eng.* **42** 1–40
Coppola L, Buoso A and Corazza F 2011 Electrical properties of carbon nanotubes cement composites for monitoring stress conditions in concrete structures *Appl. Mech. Mater.* **82** 118–23
Galao O, Zornoza E, Baeza F J, Bernabeu A and Garces P 2012 Effect of carbon nanofiber addition on the mechanical properties and durability of cementitious materials *Mater. Constr.* **62** 343–57
Gengying L and Peiming W 2005 Microstructure and mechanical properties of carbon nanotubes-cement matrix composites *J. Chin. Ceram. Soc.* **33** 105–8
Gong H, Zhang Y, Quan J and Che S 2011 Preparation and properties of cement based piezoelectric composites modified by CNTs *Curr. Appl. Phys.* **11** 653–6
Hou T C 2008 Wireless and electromechanical approaches for strain sensing and crack detection in FRC materials *PhD Dissertation* Civil and Environmental Engineering, University of Michigan, Ann Arbor, MI
Hou T C and Lynch J P 2005 Conductivity-based strain monitoring and damage characterization of fiber reinforced cementitious structural components *Proc. SPIE* **5765** 419
Khayat K H and Yahia A 1998 Simple field tests to characterize fluidity and washout resistance of structural cement grout *Cem. Concr. Aggr.* **20** 145–56
Li H, Ou J, Xiao H, Guan X and Han B 2011 Nanomaterials-enabled multifunctional concrete and structures *Nanotechnology in Civil Infrastructure* (Berlin: Springer) pp 131–73
Li H, Xiao H G and Ou J P 2006 Effect of compressive strain on electrical resistivity of carbon black-filled cement-based composites *Cem. Concr. Compos.* **28** 824–8
Li M, Lin V W, Lynch J P and Li V C 2013 Carbon black engineered cementitious composites—Mechanical and electrical characterization *Am. Conc. Inst.* **292** 1–16
Li V C 1998 Engineered cementitious composites—Tailored composites through micromechanical modeling *Fiber Reinforced Concrete: Present and the Future* (Montreal: CSCE) pp 64–97
Li V C 2002 Reflections on the research and development of engineered cementitious composites (ECC) *Proc. JCI Int. Workshop on Ductile Fiber Reinforced Cementitious Composites (DFRCC)—Application and Evaluation (DRFCC-2002) (Takayama Japan)* pp 1–21
Li V C, Wu C, Wang S, Ogawa A and Saito T 2002 Interface tailoring for strain-hardening polyvinyl alcohol-engineered cementitious composites (PVA-ECC) *ACI Mater. J.* **99** 463–72
Lin V W, Li M, Lynch J P and Li V C 2011 Mechanical and electrical characterization of self-sensing carbon black ECC *Proc. SPIE* **7983** 798316
Liu Z, Zhang Y, Liu L and Jiang Q 2013 An analytical model for determining the relative electrical resistivity of cement paste and C–S–H gel *Constr. Build. Mater.* **48** 647–55
Makar J M and Beaudoin J J 2004 Carbon nanotubes and their application in the construction industry *R. Soc. Ch.* **292** 331–42
Perez A, Climent M A and Garces P 2010 Electrochemical extraction of chlorides from reinforced concrete using a conductive cement paste as an anode *Corros. Sci.* **52** 1576–81
Raki L, Beaudoin J J, Alizadeh R, Makar J M and Sato T 2010 Cement and concrete nanoscience and nanotechnology *Materials* **3** 918–42
Sanchez F and Ince C 2009 Microstructure and macroscopic properties of hybrid carbon nanofiber/silica fume cement composites *Compos. Sci. Technol.* **69** 1310–8
Sixuan H 2012 Multifunctional graphite nanoplatelets (GNP) reinforced cementitious composites *PhD Dissertation* National University of Singapore p 167
Sobolkina A, Mechtcherine V, Khavrus V, Maier D, Mende M, Ritschel M and Leonhardt A 2012 Dispersion of carbon nanotubes and its influence on the mechanical properties of the cement matrix *Cem. Concr. Compos.* **34** 1104–13
Spragg R, Bu Y, Snyder K, Bentz D and Weiss J 2013 *Electrical Testing of Cement-Based Materials: Role of Testing Techniques, Sample Conditioning, and Accelerated Curing* (West Lafayette, Indiana: Joint Transportation Research Program, Indiana Department of Transportation and Purdue University) publication FHWA/IN/JTRP-2013/28 (doi:10.5703/1288284315230)
Şahmaran M and Li V C 2009 Durability properties of micro-cracked ECC containing high volumes fly ash *Cem. Concr. Res.* **39** 1033–43
Tombler T W, Zhou C, Alexseyev L, Kong J, Dai H, Liu L, Jayanthi C S, Tang M and Wu S Y 2000 Reversible electromechanical characteristics of carbon nanotubes under local-probe manipulation *Nature* **405** 769–72
Tyson B M, Abu Al-Rub R K, Yazdanbakhsh A and Grasley Z 2011a Carbon nanotubes and carbon nanofibers for enhancing the mechanical properties of nanocomposite cementitious materials *J. Mater. Civ. Eng.* **23** 1028–35
Tyson B M, Al-Rub R K A, Yazdanbakhsh A and Grasley Z 2011b A quantitative method for analyzing the dispersion and agglomeration of nano-particles in composite materials *Composites* B **42** 1395–403
Wen S and Chung D D L 1999 Piezoresistivity in continuous carbon fiber cement-matrix composite *Cem. Concr. Res.* **29** 445–9
Wen S and Chung D D L 2005 Strain sensing characteristics of carbon fiber cement *ACI Mater. J.* **102** 244–8
Wen S and Chung D D L 2006 Model of piezoresistivity in carbon fiber cement *Cem. Concr. Res.* **36** 1879–85
Wen S and Chung D D L 2007 Piezoresistivity-based strain sensing in carbon fiber-reinforced cement *ACI Mater. J.* **104** 171–9
Wen S and Chung D D L 2008 Effect of moisture on piezoresistivity of carbon fiber-reinforced cement paste *ACI Mater. J.* **105** 274–80
Xie P, Gu P and Beaudoin J J 1996 Electrical percolation phenomena in cement composites containing conductive fibres *J. Mater. Sci.* **31** 4093–7
Yazdanbakhsh A, Grasley Z, Tyson B and Al-Rub R K A 2011 Dispersion quantification of inclusions in composites *Composites* A **42** 75–83
Yıldırım G, Aras G H, Banyhussan Q S, Şahmaran M and Lachemi M 2015 Estimating the self-healing capability of cementitious composites through non-destructive electrical-based monitoring *NDT&E Int.* **76** 26–37
Zornoza E, Catala G, Jimenez F, Andion L G and Garces P 2010 Electromagnetic interference shielding with Portland cement paste containing carbon materials and processed fly ash *Mater. Constr.* **60** 21–32